Proceedings of the ASME 2024
International Mechanical Engineering Congress and Exposition
IMECE2024
November 17-21, 2024, Portland, Oregon

IMECE2024-145777

IMPROVED DE-BONDING OF COMPOSITE ADHESIVE JOINTS WITH BONDLINE INSERTS

Khushboo Tedlapu
Oakland University
Rochester, MI

Marco Gerini-Romagnoli
Oakland University
Rochester, MI

ABSTRACT

The demand for effective de-bondable adhesive technology enabling substrate separation under small loads has grown in recent years. Thermally Expandable Particles (TEP) can be embedded in structural adhesives to promote mechanical separation of the adherends. However, the activation of TEP additives in joints with non-metallic adherends is challenging and can result in substrate thermal damage and poor de-bonding performance, due to the low thermal conductivity and dielectric loss factor typical of plastics and polymer-matrix composites.

In this study, the effect of bondline stainless steel inserts on fully composite (Carbon Fiber Reinforced Polymer, or CFRP) bonded Single Lap Joints (SLJ) mechanical and de-bonding performance is evaluated. A centrifugal mixer is used to disperse the TEP in the adhesive. TEP additives are activated using induction heating of the bondline insert, which also helps control crack initiation and propagation. SLJ de-bonding tests are run under a constant 20 lb (89 N) load, and substrate temperature is recorded with thermocouples and an infrared thermometer. Joint strength is evaluated with quasi-static lap shear tests on a servo-hydraulic tensile test apparatus.

Preliminary de-bonding testing is performed on a broad initial set of 316 stainless steel insert designs. Out of those, the four best-performing insert geometries are chosen for the complete study. Two TEP enrichment levels (10% and 20% wt.) are investigated. The mechanical and de-bonding performance of SLJs with steel inserts is compared to TEP-only baseline fully-composite and multi-material (AA 6061 Aluminum Alloy + CFRP) joints.

The results show that bondline inserts enable fast de-bonding of fully-composite SLJs. Insert geometry and thickness affect joint de-bonding time and reliability, and can be optimized to allow for a partial recovery of lap shear strength. 100% de-bonding reliability is achieved with "block"-type inserts, with de-bonding performance similar to TEP-enriched metallic joints. Visual inspection of the fracture surfaces shows the relationship between TEP activation and crack propagation path. Discussion and conclusions are provided.

Keywords: Composite Joints; Reversible Adhesive Technology; Thermally Expandable Particles; Lap Shear Testing; De-bonding Testing

1. INTRODUCTION

Regulations focusing on fuel economy improvement and emission control are two of the main challenges facing the automotive industry today, and are driving automotive companies towards the increase of vehicle efficiency [1]. The environmental need to reduce carbon emissions is pushing the automotive sector to improve vehicle fuel economy while maintaining vehicle performance and passenger comfort [2]. To tackle these challenges and to reduce the industry's carbon footprint, initiatives such as light weighting structural components, incorporating design for disassembly to facilitate end-of-life recycling processes, and adopting circular economy principles are being employed in several manufacturing sectors [3]. Out of these initiatives, weight reduction is the main strategy to improve vehicle fuel economy. Furthermore, the recent shift towards electrification highlighted the need for reducing weight in body-in-white (BIW) and other automotive parts to compensate for the addition of heavy batteries and electric motors [4]. Using fiber-reinforced polymers (FRP) for vehicle body and favoring adhesive bonding over mechanical fastening has been shown to be an effective light-weighting strategy [5].

Adhesive bonding allows for uniform load distribution and reduces areas of stress concentration typically caused by mechanical fasteners and welds [6-7]. Consequently, adhesive bonding is gaining popularity in several manufacturing applications over traditional mechanical fastening.

However, in situations involving repair or recycling of bonded structures, it is often necessary to separate substrates and/or components. Typically, this separation process involves the application of substantial mechanical loads and high

temperatures, increasing the risk of damaging the adherends and hindering their subsequent recovery [8].

Maintenance, Repair, and Overhaul (MRO) and end-of-life (EoL) considerations are responsible for a growing demand for research into de-bondable adhesive technologies, which enable separation under minimal loading. Among the several proposed debonding techniques, the use of thermally expandable particles (TEP) has gained considerable attention over the years. Several studies have been conducted on the inclusion of TEPs in adhesive joints to assess bonding strength, durability in diverse environmental conditions, and debonding performance. Banea et al. [8], [9], [10], [11] demonstrated proof of concept and explored the effect of TEPs on epoxy and polyurethane adhesives, studying their trigger temperatures in automotive applications. Banea et al. [12] also investigated the effect of TEPs on the thermomechanical properties of a polyurethane adhesive by performing tensile tests. More studies were carried out to understand the effect of varying particle weight percentages in two different adhesive matrices with metallic substrates [8],[10]. The use of TEPs in structural adhesive bonding of multi-material single lap joints is also investigated [6].

TEP-driven debonding mainly relies on the heating of the substrates or on direct heat delivery to the bondline to activate the particles. However, in FRPs, this process faces challenges due to their low through-thickness thermal conductivity and dielectric loss factor. Typically, heat is delivered through electromagnetic induction, but the low dielectric loss factor makes it difficult to heat up the substrates effectively. Moreover, the low through-thickness conductivity of FRP complicates the transfer of heat to the bondline/ TEPs, leading to the formation of hot spots and the absence of continuous crack paths. These challenges have resulted in limited literature on research conducted using TEP-modified adhesives on fully composite joints [5].

In this paper, a novel methodology is proposed, with the aim of overcoming the limitations associated with TEP-driven de-bonding of fully composite joints. Stainless steel inserts are embedded within the adhesive layer to achieve debonding of fully composite Single Lap Joint (SLJ). Heat transfer to the bond line is promoted, and the effectiveness of the debonding process is improved. The inserts are designed to optimize joint strength and de-bonding performance, simultaneously. Debonding performance is evaluated by the debonding time.

2. MATERIALS AND GEOMETRY OF TEST SAMPLES

The fully composite bonded single lap joints (SLJ) consist of coupons made of woven carbon fiber (2x2 twill weave CFRP 0-90-0, aligned with the SLJ axes) in an epoxy matrix, with a thickness of 1.6 mm (1/16”). The geometry and material properties of the CFRP adherends are shown in Figure 1 and Table 1, respectively. The bond area measures 25.4 mm (1 in.) in length (joint overlap) by 25.4 mm (1 in.) in width. Holes are drilled into one side of the coupons to fit the SLJ in the de-bonding apparatus.

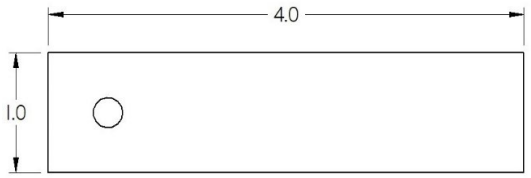

FIGURE 1: GEOMETRY OF CFRP COUPONS (DIMENSIONS IN INCHES)

TABLE 1: CFRP MATERIAL PROPERTIES

Young Modulus (GPa)	Tensile Strength (MPa)	Elongation at Break (%)
32.5	553	1.7

The adhesive used is Araldite 2015, a commercially available two-part structural epoxy adhesive. The average lap shear strength of the properly mixed baseline adhesive is approximately 12 MPa with CFRP substrates. The adhesive is modified with different weight percentages of Thermally Expandable Particles. Guided by previous studies [6, 8], the selected particle grade is Expancel 031DU40, in 10% and 20% weight concentrations. The properties of the particle additives are listed in Table 2.

TABLE 2: EXPANCEL 031DU40 PROPERTIES

Particulate Size (μm)	T_{start} (°C)	T @ Max Expansion (°C)
10 - 16	80 - 95	120 - 135

The bondline inserts are made from 316 stainless steel sheets. Preliminary (screening) de-bonding tests of various proposed insert designs are carried out on joints with mixed-material adherends (CFRP and 6061 T6 Aluminum Alloy) and 20% wt. TEP enrichment. Finally, two insert designs, here called “block” and “cage”, are chosen for their superior performance and ease of manufacturing. The geometry of the selected inserts is shown in Figure 2. “Cage”-type inserts are waterjet cut with the help of a die to minimize warping, while block-type inserts are sheared to fit the bond area of 25.4mm x 25.4mm (1” x 1”). Two thicknesses, 0.05 mm (0.002”) and 0.15 mm (0.007”), are investigated for both designs. The complete list of additives and insert combinations is shown in Table 3.

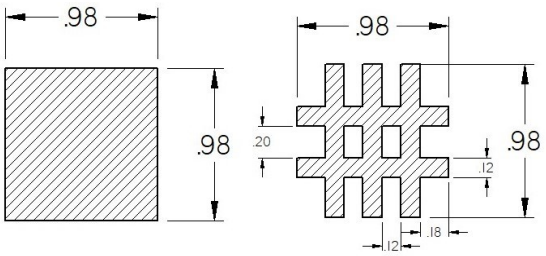

FIGURE 2: "BLOCK" AND "CAGE" INSERTS (DIMENSIONS IN INCHES)

TABLE 3: SLJ CONFIGURATIONS

Test Condition	TEP Weight Concentration (%)	Insert Type	Thickness (in.)
1	10	-	-
2	10	Block	0.007
3	10	Block	0.002
4	10	Cage	0.007
5	10	Cage	0.002
6	20	-	-
7	20	Block	0.007
8	20	Block	0.002
9	20	Cage	0.007
10	20	Cage	0.002

3. EXPERIMENTAL SETUP AND METHODOLOGY

3.1 Sample Preparation

Carbon fiber substrates are prepared for bonding by hand-scuffing the bond area with 300 grit sandpaper, followed by ultrasonic cleaning using a biodegradable solution to remove grease, oil, and residual dust from the sanding process. The TEP-modified adhesive is created by mixing two components of Araldite 2015 in a 1:1 mass ratio and incorporating Expancel 031DU40 particles at 10% and 20% weight concentrations. The particles and adhesive are combined using an automated centrifugal mixer at 2100 rpm for 90 seconds total, with a 30-second rest period after the first 45 seconds. The modified adhesive is then applied to the bond area (1" x 1") of both coupons, and the insert is sandwiched between them. A custom bonding fixture (shown in Fig. 3) ensures proper joint alignment, overlap, and bondline thickness. The joints undergo an oven-accelerated curing process at 65°C for four hours. The curing schedule is chosen to prevent undesired triggering of the TEP additives during joint manufacturing. Three samples are tested for each combination.

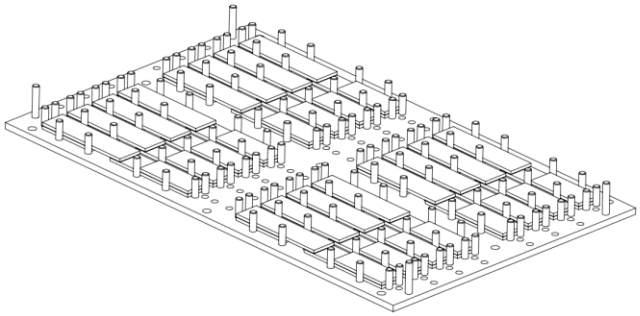

FIGURE 3: SLJ ALIGNMENT FIXTURE

3.2 De-bonding Mechanism and Test Methodology

The de-bonding tests are conducted using an RDO HFI 3.0 kW RF induction heating system with a frequency range of 135-400 kHz. The joint is positioned within the water-cooled copper helical coil shown in Fig. 4, with the SLJ bond area fully enclosed within the coil. The joint is held at one end by the fixture pin, which engages the hole shown in Fig. 1, while a constant load of 89N is applied to the other end with calibrated weight plates and a simple rope-and-pulley system. The full test setup is shown in Fig. 4. For SLJs with cage-type inserts, heating power is set at 1.5 kW at a frequency of 330 kHz, while for SLJs with block-type inserts, power is set to 0.9 kW at a frequency of 346 kHz.

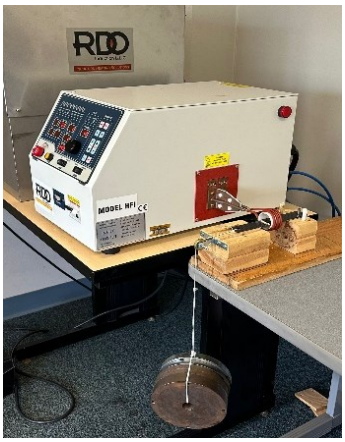

FIGURE 4: INDUCTION HEATER TEST SETUP

When the inducting heater is activated, an alternating magnetic field is generated along the coil's axis, which is aligned with the SLJ. Due to the longitudinal direction of the magnetic field, the bond line inserts are heated, while the substrates are effectively transparent to the electromagnetic waves: CFRP substrates are susceptible to induction heating when the orientation of the magnetic field is perpendicular to the weave plane, which could be achieved by using a "pancake-style" coil [13]. However, differently from joints with at least one metallic adherend, substrate heating is not an effective strategy to trigger the expansion of the TEP in the adhesive layer of fully-

composite joints, because of the poor through-thickness heat transfer properties of CFRP substrates. Substrate-driven activation of the TEPs would require heating the adherends to temperatures in excess of the point of thermal degradation of the polymeric matrix. However, by employing a helical coil, the dielectric loss factor of the CFRP substrates is negligible, and only the bondline insert is inductively heated.

Once the adhesive in close proximity to the insert reaches the expansion temperature of the TEPs, the particles expand in volume, creating and propagating a crack in the bondline, and the joint de-bonds. The time to de-bond is defined as the time between the start of the induction heating process and the joint's full separation. For the purpose of this study, if the joint fails to de-bond after 600 seconds (10 minutes), the test is halted.

3.3 Lap Shear Test Methodology

The lap shear strength of the test specimens is evaluated using the 810 MTS Testing System shown in Figure 5. ASTM Standard Test Method for Lap Shear Adhesion for Fiber Reinforced Plastic Bonding (D5868_01) is used for testing [14]. The loading rate for specimens is 12.7 mm/min (0.5"/min). Alignment tabs are used to avoid the introduction of an artificial bending moment on the joint.

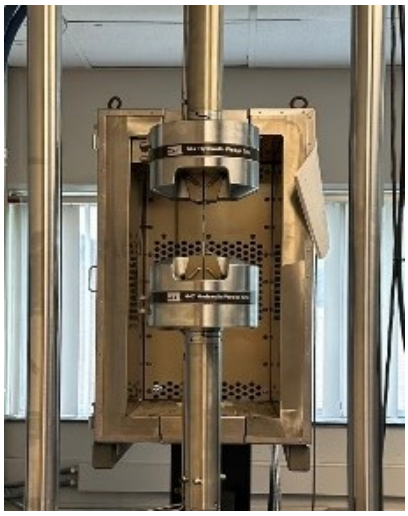

FIGURE 5: SLJ IN 810 MATERIAL TESTING SYSTEM

4. RESULTS

The results of the de-bonding and lap shear tests are presented and discussed in this section, for the 10 joint combinations listed in Table 3. Three identical joints are tested for each combination.

4.1 De-bonding Results

The effect of the 4 combinations of insert geometry and thickness, and of the TEP additive concentration on the average debonding time is shown in Figure 6. As discussed in the methodology section, a time limit of 10 minutes is set for the test, guided by previous studies [6]. Joints exceeding this limit are considered to have survived the test.

No de-bonding is observed in any of the SLJs with TEP-modified adhesive only (i.e. without inserts). Conversely, as shown in Fig. 6, joints with either "cage" or "block" inserts are able to de-bond within 600 seconds. The average time to de-bond shown in Fig.6 only includes successful de-bonding tests, with the error bars indicating 1 standard deviation (σ).

TEP Additive concentration significantly affects debonding time for "cage"-type inserts, with higher particle content resulting in quicker de-bonding (by an approximate factor of 2) compared to the lower 10% concentration samples. However, the de-bonding time of "block"-type samples is less affected by the TEP concentration: the de-bonding performance increases by an approximate factor of 1.2 when doubling the TEP concentration. This shows that heat is transferred efficiently from the "block"-type inserts to the bondline (and to the TEP additives), and that the adhesive-insert interface offers a smooth and continuous path along which the crack caused by the combined action of the TEP expansion and of the 89 N external load can propagate.

At 10% TEP concentration, joints with "block"-type inserts de-bond 3.5 times more quickly (on average) than joints with "cage"-type inserts. The gap between the de-bonding performance of "block"- and "cage"-type is significantly reduced at 20% additive concentration: joints with "block"-type inserts de-bond 2.2 times more quickly (on average) than joints with "cage"-type inserts.

Insert thickness is also found to significantly affect the de-bonding performance of the tested SLJ samples: increasing the thickness of the insert causes an increase in time to de-bond for "cage"-type samples, while it has the opposite effect for "block"-type specimens.

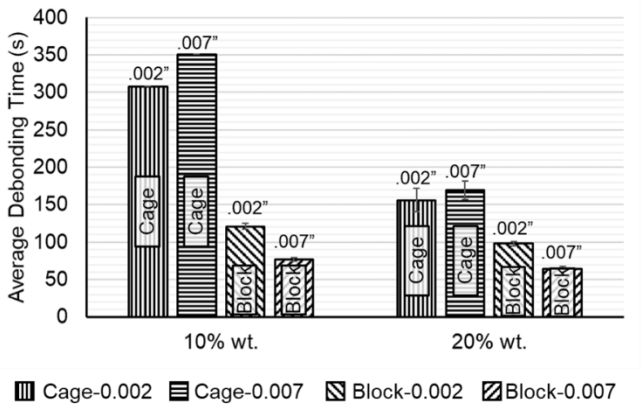

FIGURE 6: DE-BONDING PERFORMANCE OF ALL JOINT COMBINATIONS WITH "CAGE"- AND "BLOCK"-TYPE INSERTS (1σ ERROR BARS)

The de-bonding reliability of all the joint/insert combinations for the 10% and 20% wt. TEP additive concentrations is presented in Figure 7. De-bonding reliability is defined as the share of the test samples that de-bond within the 10-minute limit, with a reliability of 100% indicating that all of

the test samples de-bond successfully. Joints with "block"-type inserts successfully de-bond at both additive concentrations, while only part of the samples with "cage"-type inserts de-bond under any of the test conditions. For "cage"-type joints, de-bonding reliability increases at higher TEP additive concentration, from 33% (10% wt.) to 50% (20% wt.).

The large surface area at the insert/adhesive interface of "block"-type samples helps maximize efficient heat transfer to the adhesive layer. Moreover, this area offers a continuous path along which cracks can propagate during the de-bonding process. This results in 100% de-bonding reliability at both 10% and 20% TEP concentrations, and for both tested insert thicknesses.

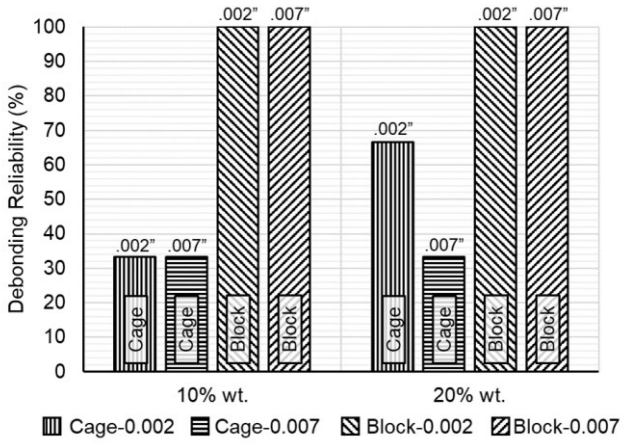

FIGURE 7: DE-BONDING RELIABILITY PERFORMANCE OF ALL JOINT COMBINATIONS WITH "CAGE"- AND "BLOCK"-TYPE INSERTS

The fracture surfaces of de-bonded "cage"-type and "block"-type samples are presented in Figs. 8 and 9, respectively. Visual inspection of all tested joints shows that de-bonding occurs primarily at the interface between the adhesive and the insert, consistently with previous studies, where joint de-bonding is observed to take place at the aluminum substrate-adhesive interface [6,8].

The geometry of the "cage"-type inserts causes checkered de-bonding hotspots to appear at the intersections of the longitudinal and transverse elements, as highlighted by the red circles in Fig. 8. Continuous crack propagation is hindered by the uneven activation of the TEP additives, as well as by the insert geometry, which creates de-bonding paths on multiple parallel planes through the bondline thickness, as shown in Fig. 8. This could explain the decrease in de-bonding performance observed in Fig. 6: thicker "cage"-type inserts may cause the cracks to grow along multiple de-bonding planes across the insert thickness, slowing down the de-bonding process, which requires continuous crack propagation.

Conversely, continuous crack growth along the insert-adhesive interface and even TEP activation are observed for samples with "block"-type inserts, as shown in Fig. 9. The fracture surface is smooth, showing continuous crack propagation along the insert, and an U-shaped pattern of activated TEPs appears on all test samples. This could show that the sides of the "block"-type insert are heated more effectively by the electromagnetic field, but further investigation is needed.

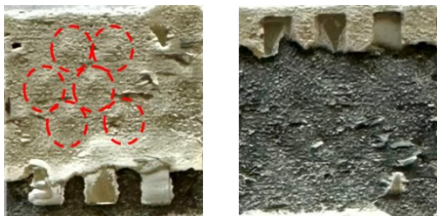

FIGURE 8: FRACTURE SURFACES OF DE-BONDED "CAGE" TYPE COUPON, WITH CIRCLED HOTSPOTS

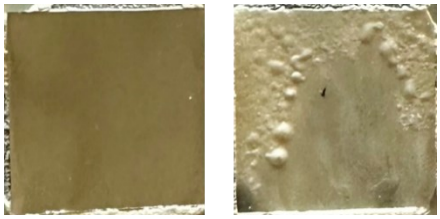

FIGURE 9: FRACTURE SURFACES OF DE-BONDED "BLOCK" TYPE COUPON, WITH U-SHAPED ACTIVATED TEP PATTERN

4.2 Lap Shear Strength Results

The average lap shear strength results for samples with baseline adhesive and TEP-modified adhesive, without the embedded stainless steel inserts, is shown in Figure 10. The inclusion of TEP additives in the adhesive layer causes a significant reduction in quasi-static lap shear strength (~17%) for fully composite SLJs. However, increasing the TEP concentration from 10% wt. to 20% wt. does not further affect the mechanical performance of the joints. This is in contrast to the results reported in the literature [6, 8-12]. However, the effect of TEP additives on joint performance is highly dependent on the adhesive properties, and further investigation of higher weight concentrations could reveal additional strength reductions.

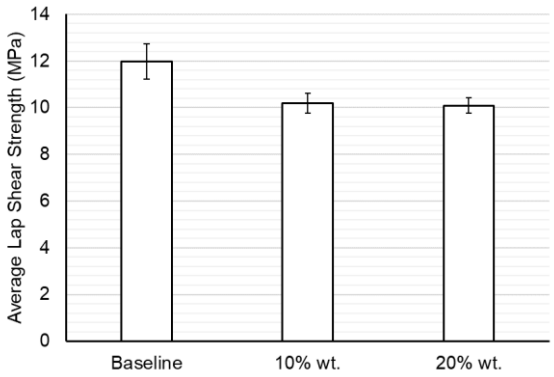

FIGURE 10: LAP SHEAR STRENGTH COMPARISON FOR BASELINE AND TEP-MODIFIED ADHESIVE

The average lap shear strength for 10% and 20% Expancel additive concentrations for joints without inserts (TEP-only) and with the tested insert designs is depicted in Figs. 11 and 12, respectively. Interestingly, the lap shear strength follows an inverse trend when compared to the time to de-bond (Fig. 6): the values of insert thickness that achieved quicker de-bonding times are also characterized by a higher lap shear strength, simplifying the choice of insert geometry for optimal strength and de-bonding performance.

Moreover, the same optimal combinations of insert geometry and thickness are responsible for significant strength recovery when compared to TEP-only joints: samples enriched with 10% wt. TEP additives, with 0.002"-thick "cage"-type inserts show a 9.3% lap shear strength improvement over TEP-only samples, while joints with 0.007"-thick "block"-type inserts demonstrate a more moderate – but still significant – 6.0% lap shear strength improvement. Similar improvements are observed for samples with 20% wt. TEP concentration: joints with 0.002"-thick "cage"-type inserts show a 10.9% improvement, and joints with 0.007"-thick "block"-type inserts exhibit an 8.9% improvement over TEP-only samples.

Data scatter is larger for "cage"-type inserts. The error bars in **Error! Reference source not found.**10 and Figure 11 represent one standard deviation (σ).

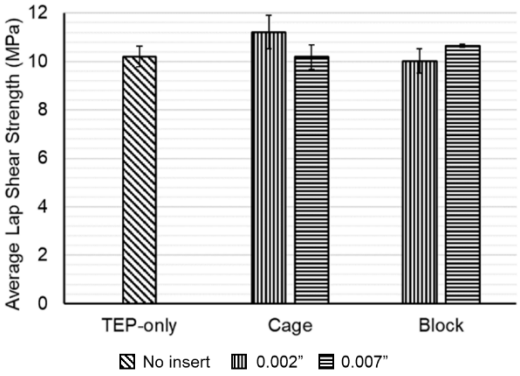

FIGURE 11: LAP SHEAR STRENGTH AT 10% TEP CONCENTRATION (1σ ERROR BARS)

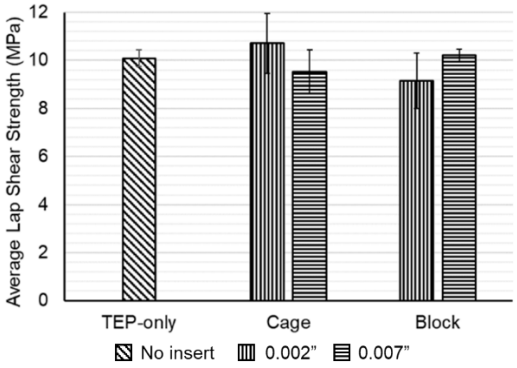

FIGURE 12: LAP SHEAR STRENGTH AT 20% TEP CONCENTRATION (1σ ERROR BARS)

4.3 Comparison between Fully Composite and Multi-Material Joints

The de-bonding performance of the fully composite joints with the proposed insert geometries is compared to multi-material (6061-T6 Aluminum Alloy substrate bonded to CFRP) joints, with 10% wt. TEP enrichment. As shown in Fig. 13, fully composite TEP-only samples do not de-bond, while multi-materials TEP-only joints de-bond in just over 80 seconds, on average. However, all of the tested combinations of insert geometry and thickness bring significant improvements in the de-bonding performance of multi-material joints, helping to concentrate induction heating within the adhesive layer. Worse de-bonding performance is observed across the board for fully composite joints; the time to de-bond for samples with 0.007"-thick "block"-type inserts, however, is within 20 seconds of the multi-material equivalent joints.

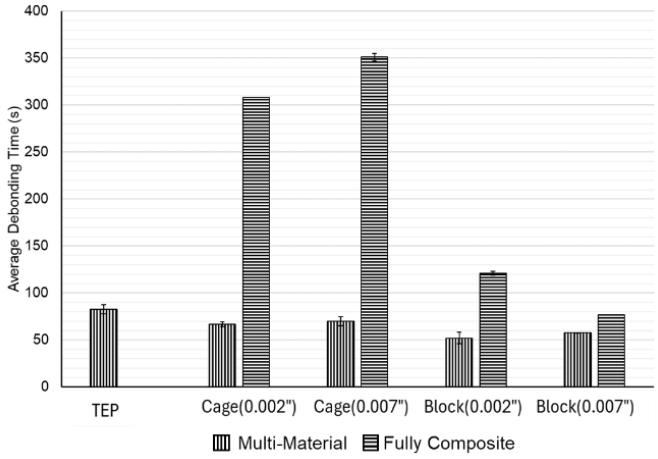

FIGURE 13: DE-BONDING TIME OF MULTI-MATERIAL VS FULLY COMPOSITE JOINTS (10% WT. TEP) FOR ALL TESTED COMBINATIONS (1σ ERROR BARS)

The lap shear strength of fully composite joints is compared to the equivalent multi-material samples in Fig. 14. The lap shear strength recovery is similar to what is shown in Fig. 11, with 0.002"-

thick “cage”-type and 0.007”-thick “block”-type inserts significantly improving the lap shear strength of TEP-modified multi-material SLJ coupons.

5. CONCLUSION

The lap shear strength and de-bonding performance of fully composite SLJs with varying additive concentration and combinations of stainless steel insert geometry and thickness are investigated and compared to TEP-only and multi-material SLJs.

All tested insert designs enable TEP-driven substrate separation of fully composite joints, which would otherwise fail to de-bond within the prescribed 600 second time limit. However, only “block”-type inserts ensure 100% de-bonding reliability, while the development of hotspots and the overall geometry of “cage”-type inserts cause the de-bonding reliability to dip below 50% on average. “Block”-type inserts are shown to promote uniform and effective heat transfer to the bondline, while providing a continuous crack propagation path during the de-bonding process.

Optimum values of insert thickness are identified for both “cage”-type (0.002”) and “block”-type (0.007”) samples, combining the shortest de-bonding time with the highest values of lap shear strength recovery (compared to TEP-only samples). The largest improvements in joint strength are observed with “cage”-type inserts: up to 11% improvement for 0.002”-thick “cage”-type samples vs 9% improvement for 0.007”-thick “block”-type specimens.

Multi-material (Aluminum/CFRP) SLJ samples are shown to benefit from any of the tested stainless steel insert designs, which help concentrate induction heating within the adhesive layer, improving de-bonding efficiency. Similar patterns of strength recovery are observed for fully composite and multi-material joints. The de-bonding time of multi-material joints is significantly lower across the board than for the equivalent fully composite counterparts.

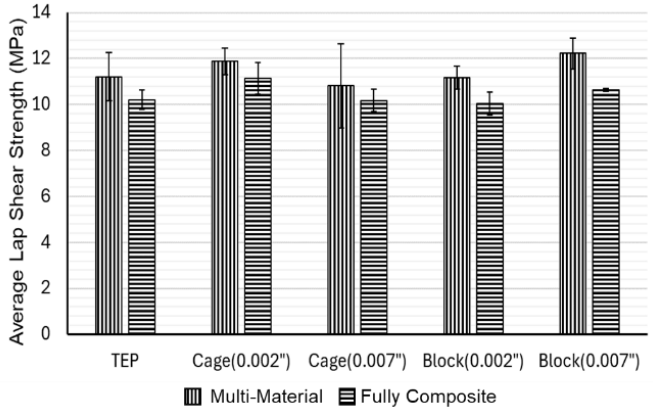

FIGURE 14: LAP SHEAR STRENGTH OF MULTI-MATERIAL VS FULLY COMPOSITE JOINTS (10% WT. TEP) FOR ALL TESTED COMBINATIONS (1σ ERROR BARS)

ACKNOWLEDGMENTS

This research study was funded by the NSF IUCRC for Composite and Hybrid Materials Interfacing (CHMI), Award # 2052658.

REFERENCES

[1]. P. K. Mallick, “Design and Manufacturing for Lightweight Vehicles”, Woodhead Publishing, 2020.

[2]. S. Modi, M. Stevens, and M. Chess, 2017, “Mixed Material Joining Advancements and Challenges", Center for Automotive Research (CAR), Ann Arbor, MI.

[3]. A. A. Gialos, V. Zeimpekis, N. D. Alexopoulos, N. Kashaev, S. Riekehr, and A. Karanika, “Investigating the impact of sustainability in the production of aeronautical subscale components”, Journal of Cleaner Production, vol. 176, pp. 785–799, March 2018, doi: https://doi.org/10.1016/j.jclepro.2017.12.151.

[4]. R. Rana, C. Lahaye, and R. K. Ray, “Overview of Lightweight Ferrous Materials: Strategies and Promises”, The Journal of The Minerals, Metals & Materials Society, vol. 66, no. 9, pp. 1734–1746, September 2014, doi: https://doi.org/10.1007/s11837-014-1126-5.

[5]. J. Goodenough, A. Fitzgerald, K. Bean, J. Hatcliffe, A. Slark, I. Hamerton, and I. Bond, “Reversible adhesives and debondable joints for fibre-reinforced plastics: Characteristics, capabilities, and opportunities”, Materials Chemistry and Physics, vol. 299, p. 127464, April 2023, doi: https://doi.org/10.1016/j.matchemphys.2023.127464.

[6]. G. Piazza, M. Burczyk, M. Gerini-Romagnoli, G. Belingardi, and S. A. Nassar, “Effect of thermally expandable particle additives on the mechanical and reversibility performance of adhesive joints”, Journal of Advanced Joining Processes, vol. 5, p. 100088, June 2022, doi: https://doi.org/10.1016/j.jajp.2021.100088.

[7]. C. Sato, R. J. C. Carbas, E. A. S. Marques, A. Akhavan-Safar, and L. F. M. da Silva, “Effect of disassembly on environmental and recycling issues in bonded joints”, Adhesive Bonding (Second Edition), Woodhead Publishing, 2021, pp. 407–436. doi: https://doi.org/10.1016/B978-0-12-819954-1.00016-2.

[8]. M. D. Banea, L. F. M. da Silva, and R. J. C. Carbas, “Debonding on command of adhesive joints for the automotive industry”, Internal Journal of Adhesion and Adhesives., vol. 59, pp. 14–20, June 2015, doi: https://doi.org/10.1016/j.ijadhadh.2015.01.014.

[9]. M. D. Banea, L. F. M. da Silva, R. J. C. Carbas, and R. D. S. G. Campilho, “Structural Adhesives Modified with Thermally Expandable Particles”, Journal of Adhesion, vol. 91, no. 10–11, pp. 823–840, Oct. 2015, doi: https://doi.org/10.1080/00218464.2014.985785.

[10]. M. D. Banea, L. F. M. da Silva, R. J. C. Carbas, and S. de Barros, “Debonding on command of multi-material adhesive joints”, Journal of Adhesion, vol. 93, no. 10, pp. 756–770, August 2017, doi: https://doi.org/10.1080/00218464.2016.1199963.

[11]. M. D. Banea, L. F. M. Da Silva, R. J. C. Carbas, D. K. K. Cavalcanti, and L. F. G. De Souza, “The effect of environment and fatigue loading on the behaviour of TEPs-modified adhesives”, Journal of Adhesion, vol. 96, no. 1–4, pp. 423–436, March 2020, doi: https://doi.org/10.1080/00218464.2019.1680546.
[12]. M. D. Banea, L. F. M. da Silva, R. J. C. Carbas, and R. D. S. G. Campilho, “Mechanical and thermal characterization of a structural polyurethane adhesive modified with thermally expandable particles”, International Journal of Adhesion and Adhesives, vol. 54, pp. 191–199, October 2014, doi: https://doi.org/10.1016/j.ijadhadh.2014.06.008.
[13]. T. Fu, J. Xu, and Z. Hui. "Analysis of induction heating temperature field of plain weave CFRP based on finite element meso model", Applied Composite Materials 28 (2021): 149-163.
[14]. ASTM, “Standard Test Method for Lap Shear Adhesion for Fiber Reinforced Plastic (FRP) Bonding”, ASTM Volume 15.06, Adhesives, 2014, doi: https://doi.org/10.1520/d5868-01r14